Distributed Blind Interference Management with Computational Antennas

Milad Johnny and Alireza Vahid

Abstract

Traditionally, wireless communication protocols and antennas are designed separately. However, there is significant potential gain in a co-design approach in which antennas and protocols complement one another. In this work, we present a new receiver antenna capable of performing simple algebraic operations in the analog domain, as well as a new communication protocol to effectively remove most of the interference signal power in K-user interference channels. The proposed hardware is a reconfigurable patch antenna in which each patch can be controlled individually using an RF switch to create huge diversity at the receiver. We exploit the space-time diversity to find two separate combinations of activating or deactivating patches to allow for interference neutralization/elimination. Finding such states is a cumbersome task for which we develop low-complexity efficient algorithms. Finally, we devise simple encoding and decoding with short pre-coder length to exploit the benefits of our designs. Our implementation does not rely on channel state information at the transmitters; works at finite signal-to-noise ratios unlike the typical degrees-of-freedom results; and works in slow-fading environments. We calculate the average achievable rates, and we provide outage analysis of our technique.

Index Terms

Interference management, average sum rate, outage capacity, reconfigurable antennas, no CSIT.

I. Introduction

The interference channel (IC) models single-hop peer-to-peer communication, and many wireless networks, such as cellular networks in which base stations communicate to mobile users, fall under this model. Other wireless networks such as microcells and femtocells can be also modeled as interference channels. In fact, moving towards denser networks and more aggressive

Alireza Vahid is with the department of Electrical Engineering at the University of Colorado Denver, USA. Authors' email addresses: mjohnny@uwaterloo.ca and alireza.vahid@ucdenver.edu.

spectrum reuse accentuates the importance of interference channels in which network capacity improvement is hampered by the interference signal power.

Unfortunately, except for special cases [1]–[4] the capacity of interference channel networks remains unknown. Broadly speaking, the Han-Kobayashi scheme [5], which uses rate-splitting, is considered to be the best achievable scheme for two-user interference channels. Especially for a class of injective deterministic interference channels, the optimality of this approach using converse proof has been demonstrated [6]. But for more than two users and for other types of interference channels, this approach does not scale. Therefore, the problem of interference in many wireless networks continues to limit network capacity and any practical interference management solution would be of great importance.

A commonly used method for handling interference is to simply avoid the problem through orthogonalization such as time/frequency division medium access (TDMA/FDMA) or code division medium access (CDMA). Unfortunately, these schemes are suboptimal and cannot support the increasing demand for higher communication data rates. Another approach to improve spectral efficiency is to use multiple antenna structures and to use joint processing at the receivers, which requires channel state information at the transmitters. To complement the previous approach, several results explore using multiple antenna structures at the receivers, which requires joint processing, several RF chains in the design, and multi-channel analog-to-digital convertors (ADCs). These characteristics add significant hardware complexity [7].

In recent years, the concept of interference alignment (IA) has been proposed as a more sophisticated form of interference management. In the context of K-user interference channels, IA achieves a sum degrees-of-freedom (DoF) of $K/2$. DoF is the pre-log factor in the expression for achievable rates and can be thought of as the equivalent number of parallel point-to-point additive white Gaussian noise (AWGN) channels inside a larger network when the signal-to-noise ratio (SNR) tends to infinity. In other words, IA shows that the number of interference-free dimensions scales linearly with the number of users. Thus, a $K/2$ DoF exhibits significant improvement over orthogonalization techniques which only achieve a DoF of 1. Although IA has a lot of theoretical benefits, there are a number of challenges and barriers in translating this method into a practical solution such as the assumption of high-resolution CSI (in some cases global perfect CSI) for the $K-$user IC, the fast-fading channel model, and long precoder lengths at the transmitters [8], [9]. These challenges cast doubt about the practicality of the IA concept.

There are different approaches to reducing the sensitivity of interference alignment to CSI.

The first one is related to accessing CSI within limited distortion [10], the second one is related to delayed CSI [11]–[15], and finally, the last one is known as blind IA (BIA) [16], [17]. The authors in [18], [19] show that in the case of blind channel knowledge or even finite precision CSI, the sum DoF of interference channel collapses to what is achievable by time or frequency sharing methods. However, this rather discouraging observation, as we show in this paper, does not mean that no gain can be obtained at finite SNR. In fact, we can fully trace the $K/2$ scaling factor within some operation SNR range.

In [16], the authors show that if the channel coherence has some specific structure, then the benefits of IA can be still attained without accessing CSI at the transmitters. To control channel coherence times, one idea is to use multi-mode switching antennas at the receivers [20], [21]. In this case, the receivers are equipped with an antenna that can switch among r different reception modes and the transmitters use specifically designed precoders to create the transmission signals. Using this approach, a sum DoF of $6/5$ is achievable in 3-user ICs. This approach is also generalized to $K-$user interference channels to show that when the number of users goes to infinity, the sum DoF goes to the value of $\sqrt{K}/2$ [17]. In [21], the authors propose a method to implement IA in a multipath fading environment based on a new receive antenna structure. However, the designs and the algorithms are complex and not practical. The scheme of [22] relies on the availability of time-varying, independent channel coefficients drawn from a discrete uniform distribution. In [23], the authors propose a scheme in which receivers create nulls in different spatial directions; while maintaining the desired signal's power above some threshold. This scheme relies on the presence of line-of-sight channels and thus, is not suitable for dense environments. Finally, to complement the efforts on receiver designs, in [24], [25] we demonstrated how to embed information in coherence time fluctuations induced by transmit antennas, which requires complex calculations to optimize the average achievable rates.

In this paper, we show it is feasible to trace the promised $K/2$ scaling gain of IA in finite SNR and in slow-fading environments. The key insight is to focus on receiver diversity for interference management, and design appropriate reconfigurable antenna structures to eliminate the interference power. More specifically, we propose an antenna with several sub-elements that can be controlled individually using RF switches creating a large number of reception states and enabling simple algebraic operations in the analog domain (hence, the name "computational antennas"). Among these reception states, some will be amenable to the interference management strategy we propose. We refer to such states as "proper channel conditions".

We quantify the relationship between the number of sub-elements and the chance for finding proper channel conditions at the receivers, and we propose an efficient search algorithm to find them. Once these states are identified, transmitters follow a simple transmission protocol and at the receivers, using the proposed antenna structure, interfering signals are (mostly) eliminated. We calculate the average achievable sum rate, provide outage analysis, and theoretically evaluate the distribution of the reception gain of the receiver antenna for each combined switching state. We show that it is possible to measure only a small number of reception sates in order to calculate the entire space at each receiver. We quantify the trade-off between the achievable rates and the complexity of different algorithms. We note that antenna implementation is complex and deserves additional efforts. This paper focuses on the benefits of incorporating the computational capabilities of antennas in communication protocol development. Thus, hardware details and RF analysis are not addressed in this manuscript.

In Section II, we provide a detailed motivation for our work, some notes on our results vis-a-vis existing literature, and an overview of our contributions. In Section III, we introduce the system model, receiver antenna structure, and some preliminaries as well as a motivating example. In Section IV, we describe our encoding and decoding strategy which is supported by a motivation example. We present the relation between the minimum number of antenna sub-elements and average transmission rate in Section V, and we also analyze the outage capacity behaviour of our network for each user in this section. We propose a search algorithm in Section VI, and we demonstrate how to find proper channel states at each receiver, and we analytically evaluate the complexity of our search algorithm. We present our numerical and simulation results in Section VII. Finally, Section VIII concludes the paper.

II. Motivation and Overview of the Contributions

Before presenting the results in great details, in this section, we provide a brief motivation and overview of our contributions. This paper provides answers to the following topics:

1) **Is there a contradiction with prior results?** It is known that the asymptotic high-SNR performance of interference channels, measured in terms of degrees-of-freedom, collapses to that of no channel knowledge if *perfect* channel state information is not available at the transmitters [26]. However, in this paper, we claim to attain the promised gains of IA, not only in the finite-SNR regime but also when no CSI is available at the transmitters. Thus, at first glance, there seems to be a contradiction. The reason why are results does not contradict any prior work is as follows.

It is important to realize that degrees-of-freedom analysis does not necessarily inform us of the finite-SNR behaviour of wireless networks. Using our proposed passive receive antenna design, we are able to provide the full benefit of IA within some *operational* SNR range, and beyond some threshold, our gains saturate. In other words, our results are in fact in agreement with [26], but for real-world SNR values, we can indeed provide significant gains.

2) **Is DoF a proper metric to measure the performance of real wireless networks?** Although

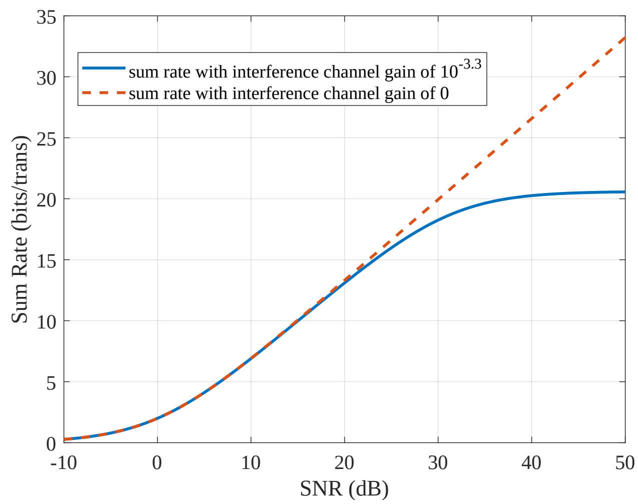

Fig. 1: Comparison between the achievable rates of perfect and imperfect alignment schemes. For practical SNR values, the imperfect alignment traces the perfect alignment scheme closely.

the DoF parameter can measure the performance of wireless networks in high SNR region, it cannot demonstrate the performance of wireless networks at applicable SNR regions. As an example consider $K-$user interference channel in which at each receiver the value of total interference signal power for all interference transmitters is a portion of desired signal power ($P_I = G_I P_d$), in this case, the total transmission rate treating interference as noise for per one reception dimension can be calculated as follows:

$$R_t\left(P_d/N\right) = \frac{K}{2}\log_2\left(1+\frac{P_d}{N+P_I}\right) = \frac{K}{2}\log_2\left(1+\frac{P_d}{N+G_I P_d}\right). \tag{1}$$

In which P_d is the desired signal power and P_I is the total interference signal power at each receiver. In this case, the value of sum DoF (d_{sum}) can be calculated as follows:

$$d_{\text{sum}} = \lim_{P_d/N\to\infty}\frac{R_t\left(P_d/N\right)}{\log_2\left(P_d/N\right)} = 0, \tag{2}$$

while d_{sum} equals to zero, for low values of α we can trace the sum rate of $K/2\log_2\left(1+P_d/N\right)$ for wide range of P_d. Figure 1 compares in a 4-user IC the perfect IA gain (sum DoF of 2) to that of an imperfect interference cancellation scheme with $G_I = 10^{-3.3}$. The imperfect scheme closely traces the perfect IA gain within a wide range of SNR values.

3) **Is it possible to reach the benefit of IA without accessing CSIT?** In this paper, we propose a strategy in which the receivers can control the reception channel gain from the environmental signals and find the proper state using a searching algorithm. With the aid of the reconfigurable antenna structures without accessing channel state information at transmitters, the receivers can control the interference signals and align most of interference signal power.

4) **How does our solution compare to joint processing structures?** It is well known that using the structure of multiple antenna at the receiver can cancel the effect of interference signals from the environment but this antenna structure needs multiple RF chains and joint processing which is very sensitive to applying proper coefficients at each RF branch. Joint processing is needed at receivers which leads to higher hardware complexity. Our propose antenna structure only needs to use a simple antenna with some RF switches to control the interference signal power at the receiver. Also, it doesn't need joint processing at receiver and uses only one RF chain which reduces the price of deployment in any application.

III. System Model and Proposed Receiver Antenna Structure

In this paper, we consider a multi-cell communication system modeled as a K-user interference channel with no cooperation among the transmitters. In other words, transmitters do not exchange any data with each other. All the transmitters equipped with a simple antenna that can be used for today wireless networks, such as Omni-directional or directional antennas to have more transmission gain and lower interference generation for a local reception zone. We assume that each receiver is equipped with an antenna structure we propose in this paper.

A. Antenna Structure

Fig. 2a shows an example of our antenna with $M = 32$ sub-elements and one RF chain. The goal of the proposed antenna is to find some states across which the interfering signals can be aligned in a subspace linearly independent of the desired signal. Implementing this reception structure can drastically increase the transmission rates without channel state information at the transmitters. Fig. 4 shows an interference network with 3 users in which receivers are equipped with the proposed antenna each with $M = 8$ sub-elements. The receiver can control the RF switches to scan through and to create 2^M different states and perform simple algebraic operations as we discuss later. Further, in the receiver antenna, all elements are connected to a power combiner using RF switches. Basically, the role of these RF switches is to connect the power combiner network to each of the elements or to a match load. When an RF switch is in the active state, the power combiner network is connected to its corresponding element and it can receive the RF signal from the environment. When an RF switch is in the inactive mode, the power combiner network and antenna sub-element are connected to a passive match load (R_L), and the power combiner is disconnected from environmental signals, see Fig. 2b. All sub-elements are connected through a power combiner, the signals are filtered, amplified, and down-converted using a single RF chain as in Fig. 2b. Thus, there is no need to implement several RF chains in the proposed structure. This antenna may be modified depending on practical constraints and limitations. Therefore, the proposed antenna structure is not the only structure that may be used to achieve our goals, but the preferred design would possess the following characteristics:

- The antenna sub-elements should be distributed with distances no less than $\lambda/2$ to receive the RF signals without affecting each other (coupling) and increase spatial diversity.
- The receiver sub-elements can be orientated or fed in a semi-random manner to increase polarization diversity.
- The receiver can control these elements using M separate RF switches.
- When inactive, both the sub-element and the RF feed should be connected to match load. The first one cancels scattering from adjacent sub-elements and the second one cancels reflection from the RF network.

We now discuss how the random orientation of the sub-elements helps the receivers to gain more linearly independent equations from the transmitters. Each element of the receiver antenna has a random orientation with the reception gain of $A(\theta-\theta_i, \phi-\phi_i)$, $1 \leq i \leq M$, where θ_i and ϕ_i indicate the angular position of each element and variables θ and ϕ indicate the reception gain dependence on the direction from each element of the antenna.

For our antenna structure, since all sub-elements are on the same plane, all of them have the same elevation orientation angle. In other words, we have $\phi_1 = \phi_2 = \cdots = \phi_M$, but each sub-element has a random azimuth orientation angle. For instance in Fig. 3, two sub-elements with random orientations of θ_1 and θ_2 have been depicted. The receive signal is the function of antenna orientation angle, for Fig. 3(a), the received signal has the following form:

$$A(\theta_1 - \theta^{(1)}, \phi^{(1)})S_1 + A(\theta_1 - \theta^{(2)}, \phi^{(2)})S_2, \tag{3}$$

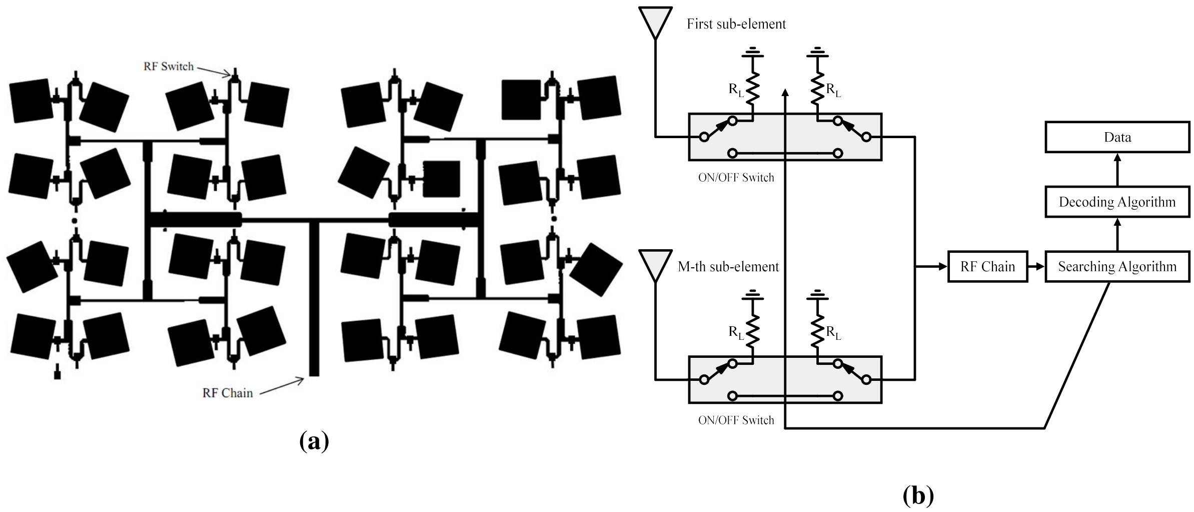

Fig. 2: (a) Receiver patch antenna structure with random orientations alongside RF combiners and RF switches; (b) the receiver can control the reception mode of its antenna.

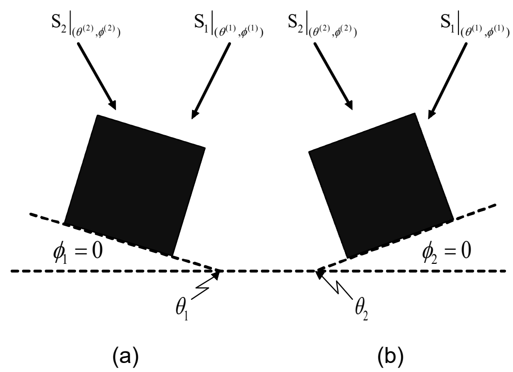

Fig. 3: Two separate sub-elements of the receiver antenna with random orientation.

and for Fig. 3(b), the received signal is:

$$A(\theta_2 - \theta^{(1)}, \phi^{(1)})S_1 + A(\theta_2 - \theta^{(2)}, \phi^{(2)})S_2, \tag{4}$$

and these equations are linearly independent. Therefore, random orientation of each element leads to generation of different linear combinations of the received signals. In practice, signals arrive from multiple paths which generates different reception gains for different antenna sub-elements.

Remark 1: In our designs, no joint processing is performed at the receivers, and the antenna structure does not have the typical hardware and software complexity of multiple input antenna structures used in single-input multiple-output (SIMO) and multiple-input multiple-output (MIMO) transceivers. We further note that the antenna is not used for receiver beamforming.

B. System Model

We consider a $K-$user interference channel (IC) with K transmitters TX_k, and K receivers $\mathrm{RX}_k, k \in \mathcal{K} = \{1, \ldots, K\}$. Each receiver is equipped with the antenna structure described in the previous subsection. Each element of the receiver antenna receives a signal from all of the transmitters. In Fig. 2a, each receiver antenna consisted of $M = 32$ squared patch elements which are connected using 32 switches and a power combiner. We can model the reception state of each receiver antenna by $M-$tuple of $S^{[j]} = (s_1^{[j]}, \ldots, s_M^{[j]}), s_i \in \{0, 1\}$.

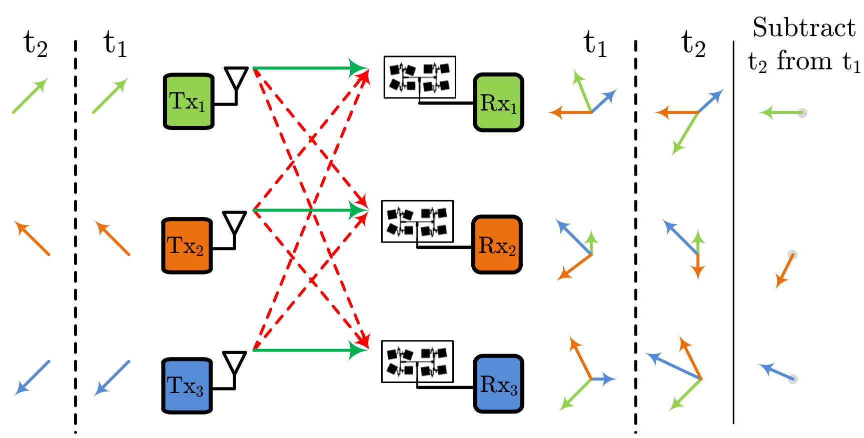

Fig. 4: A 3-user IC in which receivers are equipped with the proposed structure each with $M = 8$ sub-elements. Encoding and decoding of this example are discussed in Section IV-D.

IV. Transmission Strategy

A. Encoding strategy

We consider the problem of data transmission in an unknown time variant channel. We assume that each transmitter uses a digital modulation scheme in which Q different symbols can be transmitted through selecting a single symbol from a set of $\mathcal{S} = \{S_1, S_2, \ldots, S_Q\}$. As an example for FSK modulation, we have:

$$U_i\left(t\right) = A \cos\left(2\pi (f_c + (i-1)\Delta f) t\right),\ 0 \leq t \leq T_s,\ 1 \leq i \leq Q, \tag{5}$$

where f_c indicates modulation frequency, T_s is the symbol duration and $\Delta f = f_j - f_{j-1}$. By considering $\mathcal{E}$ as the energy of each symbol, the parameter A is equivalent to $\sqrt{\frac{2\mathcal{E}}{T_s}}$.

We assume symbols (or messages) are uniformly distributed. Transmitter TX_i wishes to send uniformly distributed message $W^{[i]} \in \mathcal{W}^{[i]}$ to RX_i, $i \in \mathcal{K}$, over n uses of the channel with time duration of nT_s. The transmission rate for the above digital modulation technique can be calculated from the following relation:

$$R^{[i]} = \frac{\log_2 Q}{T_s},\ |\mathcal{W}^{[i]}| = 2^{nR^{[i]}}. \tag{6}$$

We assume that the messages at all the transmitters are independent from each other and the channel gains. Each transmitter is subject to the total average transmission power constraint of $P_t = \frac{\mathcal{E}}{T_s}$. Transmitter TX_i encodes its message $W^{[i]}$ using the encoding function $X^{[i]}(t) = e_i\left(W^{[i]}\right)$ where $i \in \mathcal{K}$ and $e_i\left(W^{[i]}\right)$ is an one to one function from messages to the stream of symbols at TX_i. In more simple notation we have the following relation:

$$X^{[i]}(t) = e_i\left(W^{[i]}\right) = \sum_j U_{i_j}\left(t - jT_s\right),\ 1 \leq i_j \leq Q \tag{7}$$

where $U_{i_j}\left(t - jT_s\right)$ represents transmission symbol in j^{th} transmission time.

Definition 1: We define the transmission block of $B_i, i \in \{1, \ldots, n\}$ in which all transmitters repeat their transmission symbols 2 times. Therefore the total transmission time of each block is $2T_s$ and for k^{th} transmitter we can assume that $U_{k_1} = U_{k_2}$. Therefore, in this case the transmission rate of equation 6 can be calculated as $R^{[i]} = \frac{\log Q}{2T_s}$.

B. Received Signal Model

The output of each of the encoder functions from different transmitters is sent through a channel that has unknown impulse response at different sub-elements of the receiver antennas, and the noise power is added to the received signal. Thus, the received signal depends on the state of the switches at RX_i as given by:

$$Y^{[i]}(t) = \sum_{k \in \mathcal{K}} \sum_{m=1}^{M} s_m^{[i]} h_{mk}^{[i]}(t) X^{[k]}(t) + Z^{[i]}(t), 1 \leq m \leq M,\ s_m^{[i]} \in \{0, 1\} \tag{8}$$

where $s_m^{[i]}$ represents the state of the m^{th} RF switch, $\mathcal{K}$ indicates the subset of active transmitters at B^{th} transmission block and $h_{mk}^{[i]}(t)$ shows channel coefficient between TX_k, and m^{th} subelement of the receiver antenna at $\mathrm{RX}^{[i]}$. For simplicity of notation, we can define the channel coefficient vector as follows:

$$\bar{\mathbf{H}}^{[ik]} = \left[h_{1k}^{[i]}, h_{2k}^{[i]}, \ldots, h_{Mk}^{[i]}\right],\ k \in \mathcal{K}. \tag{9}$$

where all the channel coefficients at the baseband have real values with specific distribution.

Remark 2: In practice, channel values are complex. Our results extend to this case as the real and the imaginary parts can be analyzed independently. Therefore, for simplicity, we assume real-valued channel gains. For our antenna, we could use independent RF networks and switches, as well as an oscillator with a 90-degree phase-shifted version for down-converting.

C. Decoding Strategy

We assume that each receiver RX_i is aware of its channel state information and decodes its intended message $W^{[i]} \in \mathcal{W}^{[i]}$ using the decoding function $\hat{W}^{[i]} = \phi_i\left(\bar{\mathbf{Y}}^{[i]}, \mathrm{SI}_{\mathsf{Rx}_i}\right)$, where $\mathrm{SI}_{\mathsf{Rx}_i}$ is the side information available to the receiver (in this case CSI). Then, the decoding error probability at receiver RX_i is given by

$$\lambda_e^{[i]}(n) = \sum_{W^{[i]} \in \mathcal{W}^{[i]}} P\left(W^{[i]}\right) \Pr\left(\hat{W}^{[i]} \neq W^{[i]}\right) = \mathbb{E}\left[\Pr\left(\hat{W}^{[i]} \neq W^{[i]}\right)\right], \tag{10}$$

where the expectation is over the random choice of messages. The j^{th} receiver has access to channel gains $h_{mk}^{[j]}, 1 \leq m \leq M, k \in \mathcal{K}$. Therefore, each receiver has only access to the channel gains connected to it. At the end of training signal transmission phase, all the receivers by the aid of a searching algorithm find two different reception states, $S^{[j]}(i_1)$ and $S^{[j]}(i_2)$, such that they satisfy the following conditions at RX_j:

$$\sum_{k \in \mathcal{K}} |\sum_{m=1}^{M} s_m^{[j]}(i_1) h_{mk}^{[j]} - \sum_{m=1}^{M} s_m^{[j]}(i_2) h_{mk}^{[j]}| \leq \delta,\ \ k \neq j, \tag{11}$$

$$|\sum_{m=1}^{M} s_m^{[j]}(i_1) h_{mj}^{[j]} - \sum_{m=1}^{M} s_m^{[j]}(i_2) h_{mj}^{[j]}| \geq \Delta_j, \tag{12}$$

where $s_m^{[j]}(i) \in \{0,1\}$ indicates the switching state at m^{th} sub-element of j^{th} receiver at i^{th} time snapshot. The ineuality of (11) indicates that all the cross links in the two separate states of $S^{[j]}(i_1)$ and $S^{[j]}(i_2)$ have the same value to within a small value δ. Relation (12) indicates that the difference of all the direct links in two separate state of $S^{[j]}(i_1)$ and $S^{[j]}(i_2)$ is greater than Δ_j. When $\left(\frac{\Delta_j}{\delta}\right)^2$ has larger value, the portion of desired signal power to the interference signal power at RX_j has greater value. Both relations (11) and (12) can be expressed without subtraction equations as follows:

$$\sum_{k \in \mathcal{K}} |\sum_{m=1}^{M} \gamma_m^{[j]}(i_1) h_{mk}^{[j]}| \leq \delta,\ \ k \neq j \tag{13}$$

$$|\sum_{m=1}^{M} \gamma_m^{[j]} h_{mj}^{[j]}| \geq \Delta_j, \tag{14}$$

where $\gamma^{[j]} \in \{-1, 0, 1\}$. Therefore, we have 3^M different reception states to control the receiver antenna. Intuitively, if all the direct links change (the transmission link between TX_i and RX_i)

and all the cross links (the transmission link between TX_i and $\mathrm{RX}_{i'}$ where $i \neq i'$) remain the same with the small value of δ, the receivers can decode their desired symbols by a simple subtraction of two sequential received signal at each block. We accomplish this goal by finding proper reception states using the proposed antenna structure.

D. 6-*user example*

As a motivating example consider a 6-user fully-connected interference channel in which transmitters and receivers are placed randomly as specified in Appendix A. We assume each receiver is equipped with the antenna of Fig. 2b with $M = 16$ sub-elements. We further assume that all the sub-elements are omni-directional with 0 dB gain, and the following positions:

$$\left(x_r^{[k]} + \frac{\lambda}{2}i, y_r^{[k]} + \frac{\lambda}{2}j, z_r^{[k]}\right), 0 \leq i, j \leq 3,\ 1 \leq k \leq 3. \tag{15}$$

where $\left(x_r^{[k]}, y_r^{[k]}, z_r^{[k]}\right)$ indicates the position of the k^{th} receiver ($1 \leq k \leq 6$). In this case, we assume all the antenna sub-elements are located on a 4×4 square mesh. For simplicity, we assume each transmitter has a simple omni-directional antenna at $\left(x_t^{[k]}, y_t^{[k]}, z_t^{[k]}\right)$. We assume free space attenuation and phase shifting equations can model the channel gains among transceivers antennas as follows:

$$h_{ml}^{[k]} = \left(\frac{\lambda}{4\pi d_{ml}^{[k]}}\right) e^{-\frac{2\pi}{\lambda} d_{ml}^{[k]}\sqrt{-1}} \tag{16}$$

where $d_{ml}^{[k]}$ and $h_{ml}^{[k]}$ indicate the distance and the channel value between TX_l and m^{th} element of k^{th} receiver, respectively. Setting the following switch combinations:

$$\begin{aligned}
\bar{\gamma}_{\mathrm{Re}}^{[1]} &= (-1, 0, 1, -1, -1, 1, 1, -1, 1, 1, 0, 0, 0, -1, 1, 0)\,, \\
\bar{\gamma}_{\mathrm{Im}}^{[1]} &= (-1, -1, -1, 0, -1, 0, 0, 1, 1, -1, -1, 1, -1, -1, 0, 1)\,,
\end{aligned} \tag{17}$$

for the real and the imaginary parts at the first receiver, respectively, we can achieve a signal-to-interference-plus-noise ratio (SINR) of $31.22\mathrm{dB}$ for inphase and $32.62\mathrm{dB}$ for quadrature parts of the received signals. On the other hand, simply adding up the received signals at the sub-elements and treating interference as noise (TIN) at the receivers, results in SINR of $-21.53\mathrm{dB}$, $9.62\mathrm{dB}$ and $11.93\mathrm{dB}$ at the first, second, and third receivers, respectively. Thus, our new scheme drastically improves the achievable rates.

Fig. 5 shows the achievable rates of different schemes when the transmitters have the same power. In this figure, the red dashed line is the performance of treating-interference-as-noise

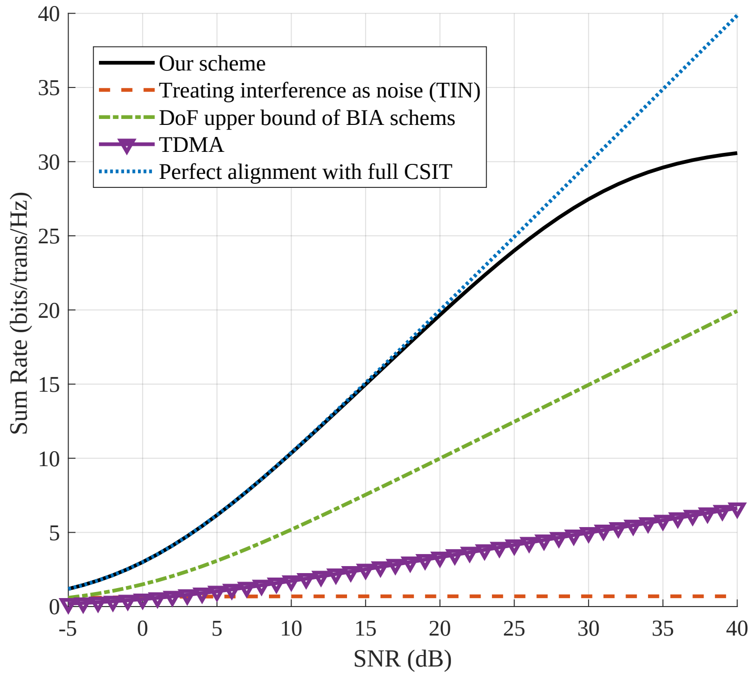

Fig. 5: A comparison between different transmission schemes with channel coefficients which are extracted from the transmitters/receivers positions and simple free space calculation.

(TIN). Since the transmitters have the same power, TIN is not the best solution here. The inverse triangle solid purple curve is the achievable rate of an orthogonalization strategy such as TDMA and is equivalent to the capacity of a single point-to-point channel. The doted dashed green curve shows the upper bound achievable DoF of the BIA scheme presented in [17] given by $d_{\text{sum}} = \frac{Kr}{r^2-r+K} = \frac{3}{2}, r = 2, K = 6$. The doted blue curve indicates the upper bound of achievable DoF for 6-user interference channel with the sum DoF of 3. Finally, the solid black curve corresponds to our transmission and reception strategy with the switching states indicated earlier. Thus, for a wide operational SNR range, our scheme significantly outperforms these other schemes. As we discuss later in Section V-B, our gains saturate at high SNR.

E. Further Assumptions

Let λ denote the wavelength of the signal. At each receiver antenna structure, sub-elements are placed at least a minimum distance of $\frac{\lambda}{2}$ from their neighbours to have channel values which are independent. Therefore, we can assume that all the channel values of $h_{mk}^{[i]}(t)$ are independent of each other and at each receiver, we have $K \times M$ different channel coefficients which are independent. In this paper, we assume cellular communication network with frequency reuse factor of $N = i^2 + ij + j^2,\ i, j \in \mathbb{W}^1$ in which each receiver is affected by many interference signals. In this case, the distance of the closest interfering transmitter to the center of each cell can be calculated from the $D = R\sqrt{3N}$ where R is the radius of each cell [27]. The minimum ratio of the desired signal-to-interference power from one interfering source is given by:

$$\mathrm{SIR} = \left(\frac{D}{R}\right)^{\alpha} = (3N)^{\frac{\alpha}{2}}\ , \tag{18}$$

where α is path loss exponent, which for the free space environment equals to 2 and for more practical cases, is greater than 2. For instance, in urban areas α ranges from 3 to 4.

V. Number of sub-elements vs. transmission rates

In this section, we evaluate the minimum number of sub-elements in our antenna structure to guarantee $\frac{\Delta^2}{\delta^2}$ is large enough for successful decoding at the receivers. The minimum number of required receiver elements and the switching modes is a function of $\delta_{\max}$ and the channel variance of σ_H^2. The channel variance parameter of σ_H^2 can be calculated from the following relation:

$$\sigma_H^2 = \int_{-\infty}^{\infty} h^2 f_H(h) dh, \tag{19}$$

wherein the above equation h is the channel value and $f_H(h)$ represents channel distribution. For simplicity of our analysis, we consider the real-valued base-band channel model. Then, we generalize the results to complex channel values.

The following lemma (proof in Appendix B) plays an important role in our analysis.

Lemma 1: If $\bar{\mathbf{H}}^{[ij]}$ *is the channel vector between* TX_j *and* RX_i *where all its elements are statistically independent, then, for a given vector* $\bar{\gamma}^{[i]}$ *whose elements are drawn randomly and independently from* $\{-1, 0, 1\}$*, the value of* $\bar{\mathbf{H}}^{[ij]}.\bar{\gamma}^{[i]}$ *has the following average variance:*

$$\bar{\mathrm{var}}\left(\bar{\mathbf{H}}^{[ij]}.\bar{\gamma}^{[i]}\right) = \frac{M}{2}\sigma_H^2 \triangleq V \tag{20}$$

where $\bar{\mathbf{H}}^{[ij]}.\bar{\gamma}^{[i]}$ *is the inner product between two vectors of* $\bar{\mathbf{H}}^{[ij]}$ *and* $\bar{\gamma}^{[i]}$ *of the same size.*

The distribution of $\bar{\mathbf{H}}^{[ij]}.\bar{\gamma}^{[i]}$ has a symmetric bell shape. A simple histogram of this parameter with $M = 10$ is plotted in Fig. 7. Based on the following lemma (proof in Appendix C), this distribution can be approximated with a zero-mean Gaussian distribution with similar variance.

[1]Whole numbers or non-negative integers

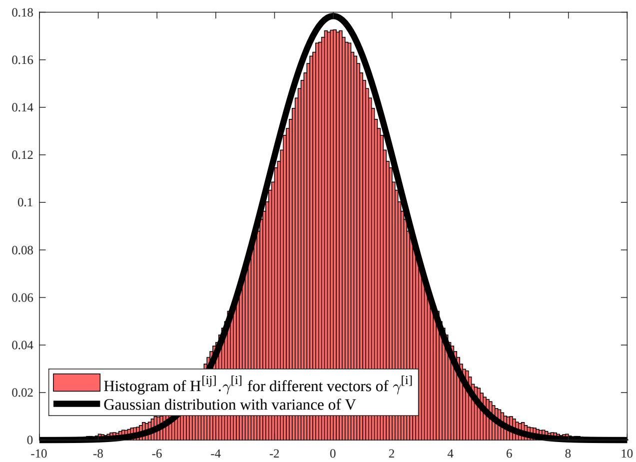

Fig. 6: Comparison between a Gaussian distribution with zero mean and variance $V = \frac{\sum_{l=0}^{M}\binom{M}{l}(M-l)}{2^M}\sigma_H^2$ and distribution of $\bar{\mathbf{H}}^{[ij]}.\bar{\gamma}^{[i]}$ for different $\bar{\gamma}^{[i]}$'s.

Lemma 2: For small enough positive values of δ, the probability of finding a vector $\bar{\gamma}^{[i]}$ to satisfy $|\bar{\mathbf{H}}^{[ij]}.\bar{\gamma}^{[i]}| < \delta$ can be approximated by $\frac{2}{\sqrt{2\pi}}\frac{\delta}{V} - \frac{2}{3\sqrt{2\pi}}\frac{\delta^3}{V^3} + O\left(\frac{\delta^5}{V^5}\right)$ for $\sigma = \sqrt{V}$ where V is defined in (20).

Since δ is small, we can ignore the effect higher order terms of $\frac{\delta}{\sigma}$. Therefore, we can assume that:

$$p\left(|\bar{\mathbf{H}}^{[ij]}.\bar{\gamma}^{[i]}| < \delta\right) \approx \frac{2}{\sqrt{2\pi}}\frac{\delta}{\sigma} = \frac{2}{\sqrt{\pi M}}\frac{\delta}{\sigma_H}. \tag{21}$$

Therefore, in this case the probability of finding two different switching states of $S^{[i]}(k_1)$ and $S^{[i]}(k_2)$ at RX_i in which the values of $\sum_{m=1}^{M} s_m^{[i]}(k_1)h_{mj}^{[i]}$ and $\sum_{m=1}^{M} s_m^{[i]}(k_2)h_{mj}^{[i]}$ are within the value of $\delta_{\max}$ can be approximated as follows:

$$p\left(|\bar{\mathbf{H}}^{[ij]}.\bar{\gamma}^{[i]}| < \delta_{\max}\right) \approx \frac{2}{\sqrt{\pi M}}\frac{\delta_{\max}}{\sigma_H},\ i \text{ is constant} \tag{22}$$

The probability of satisfying the above condition for all the cross links at RX_i in the active set of $\mathcal{K}$ can be approximated as follows:

$$p\left(|\bar{\mathbf{H}}^{[ij]}.\bar{\gamma}^{[i]}| < \delta_{\max}\right) \approx \left(\frac{2}{\sqrt{\pi M}}\frac{\delta_{\max}}{\sigma_H}\right)^{|\mathcal{K}|-1}, j \in \mathcal{K}. \tag{23}$$

A. Determining the minimum required number of sub-elements M

In this subsection, using the previous lemmas, we determine the minimum number of antenna sub-elements to satisfies our interference alignment scheme within a maximum threshold of $\delta_{\max}$. In other words, we find M such that almost surely we have $|\bar{\mathbf{H}}^{[ij]}.\bar{\gamma}^{[i]}| < \delta_{\max}$.

Lemma 3: The minimum number of M to almost surely satisfy $|\bar{\mathbf{H}}^{[ij]}.\bar{\gamma}^{[i]}| < \delta_{\max}$ is

$$\frac{|\mathcal{K}|-1}{\log 3}\log\left(\frac{\sigma_H}{\delta_{\max}}\right)+c, \tag{24}$$

where c is a function of M and for practical scenarios not greater than 1.5.

Proof: We have 3^M different reception states. In order to, with high probability, align interference signal power at RX_j, *i.e.* satisfy (13) and (14) with high probability, we need:

$$3^M\left(\frac{2}{\sqrt{\pi M}}\frac{\delta_{\max}}{\sigma_H}\right)^{|\mathcal{K}|-1} > 1, \tag{25}$$

resulting in

$$M > \frac{|\mathcal{K}|-1}{\log 3}\log\left(\frac{\sqrt{\pi M}\sigma_H}{2\delta_{\max}}\right). \tag{26}$$

In particular, if $M \leq 32$ (due to practical limits), we can relax the right hand-side of the above inequality as $M > \frac{|\mathcal{K}|-1}{\log 3}\log\left(\frac{\sigma_H}{\delta_{\max}}\right)+1.5\left(|\mathcal{K}|-1\right)$. We can conclude that all each receiver should have a minimum number of $\left\lceil\frac{|\mathcal{K}|-1}{\log 3}\log\left(\frac{\sigma_H}{\delta_{\max}}\right)+1.5\left(|\mathcal{K}|-1\right)\right\rceil$ elements to align interference signals within the value of $\delta^2_{\max}$. ■

We can rearrange (26) to obtain a bound on $\delta_{\max}$ based on the number of sub-elements:

$$\delta_{\max} < 2^{-\left(\frac{M}{|\mathcal{K}|-1}-1.5\right)\log 3}\sigma_H. \tag{27}$$

Example: As an example consider we have $|\mathcal{K}| = 4$ active transmitters and assume that $\delta_{\max} = 0.1$ and $\sigma^2_H = 1$. In this case, the minimum number of sub-elements in the receiver antenna structure (M) equals to 11. We note that in a cellular network, we typically expect interference from a small number of nearby base-stations and $|\mathcal{K}| = 4$ is a reasonable assumption.

B. Average achievable sum-rate

Denote the (physical) distance from transmitter TX_j to RX_k with d_{kj}. Then, the average achievable sum-rate can be calculated by treating as noise the total remaining interference power after the decoding strategy as follows:

$$C^{[k]}_{\mathrm{avg}} = \int_{-\infty}^{+\infty}\frac{1}{4}\log\left(1+\frac{\delta^2 P_t/d^\alpha_{kk}}{P_n+\delta^2_{\max}\left(\sum_j\frac{1}{d^\alpha_{kj}}\right)P_t}\right)f_\Delta(\delta)d\delta, j \neq k, j \in \mathcal{K} \tag{28}$$

where α is the path loss exponent coefficient, P_n is additive noise power, and from the first lemma $f_\Delta(\delta)$ is Gaussian distribution with zero mean and the variance of $\frac{M}{2}\sigma^2_H$. The coefficient $\frac{1}{4}$ comes from the transmission in two time snapshots and the basic coefficient of channel capacity for point to point communication. For a cellular communication network, we can substitute d_{kk} and d_{kj} with R and $R\sqrt{3N}$, respectively where R is the maximum cell radios and $R\sqrt{3N}$ is interference signal distance from the receiver. So, we can change the above equality with the following inequality:

$$C_{\text{avg}}^{[k]} \geq \int_{-\infty}^{+\infty} \frac{1}{4} \log \left(1 + \frac{\delta^2 P_t / R^\alpha}{P_n + \delta_{\max}^2 \left(\sum_j \frac{1}{(R\sqrt{3N})^\alpha} \right) P_t} \right) f_\Delta(\delta) d\delta, \;\; j \neq k, j \in \mathcal{K}. \tag{29}$$

If all interfering transmitters have the same distance to the receiver, and $P_t >> P_n$, then the above inequality can be simplified as follows:

$$C_{\text{avg}}^{[k]} \geq \int_{-\infty}^{+\infty} \frac{1}{4} \log \left(1 + \frac{\delta^2 P_t / R^\alpha}{P_n + \delta_{\max}^2 \left(\frac{|\mathcal{K}-1|}{(R\sqrt{3N})^\alpha} \right) P_t} \right) f_\Delta(\delta) d\delta, \;\; j \neq k, j \in \mathcal{K}. \tag{30}$$

$$\overset{(a)}{\approx} \int_{-\infty}^{+\infty} \frac{1}{4} \log \left(\frac{\delta^2 (3N)^{\frac{\alpha}{2}}}{\delta_{\max}^2 (|\mathcal{K}| - 1)} \right) f_\Delta(\delta) d\delta \tag{31}$$

$$= \int_{-\infty}^{+\infty} \frac{1}{4} \log \left(\delta^2 \right) f_\Delta(\delta) d\delta + \frac{1}{4} \log \left(\frac{(3N)^{\frac{\alpha}{2}}}{\delta_{\max}^2 (|\mathcal{K}| - 1)} \right), \tag{32}$$

where (a) comes from the assumption that $P_t >> P_n$.

Remark 3: Here, we make the assumption that $P_t >> P_n$ in order to simplify the expression for the saturation point (the point beyond which we do not follow the pre-log factor of $K/2$), and obtain some insights as we discuss below. The motivation for this assumption is that at saturation point, interference power is the main bottleneck for communications.

From the above equations and (27) where $\delta_{\max} < 2^{-\left(\frac{M}{|\mathcal{K}|-1} - 1.5\right) \log 3} \sigma_H$, we can conclude that:

$$C_{\text{avg}}^{[k]} \geq \int_{-\infty}^{+\infty} \frac{1}{4} \log \left(\delta^2 \right) f_\Delta(\delta) d\delta + \left(\frac{M}{2(|\mathcal{K}| - 1)} - \frac{1.5}{2} \right) \log 3 + \frac{\alpha}{8} \log 3N - \frac{1}{4} \log \left((|\mathcal{K}| - 1) \sigma_H \right), \tag{33}$$

considering $\sigma_H = 1$ the total average capacity of C_{avg} can be lower bounded by $|\mathcal{K}| C_{\text{avg}}^{[k]}$ as follows:

$$C_{\text{avg}} \geq \int_{-\infty}^{+\infty} \frac{|\mathcal{K}|}{4} \log \left(\delta^2 \right) f_\Delta(\delta) d\delta + \frac{M - 1.5(|\mathcal{K}| - 1)}{2} \log 3 + \frac{\alpha |\mathcal{K}|}{8} \log 3N - \frac{|\mathcal{K}|}{4} \log \left(|\mathcal{K}| - 1 \right) \tag{34}$$

In the above lower-bound, we have four terms that can be interpreted as follows:

- $\int_{-\infty}^{+\infty} \frac{|\mathcal{K}|}{4} \log \left(\delta^2 \right) f_\delta(\delta) d\delta$: This term captures the multi-path gain of the environment at the antenna, see Fig. 7. We note that with beamforming, such gains would disappear;

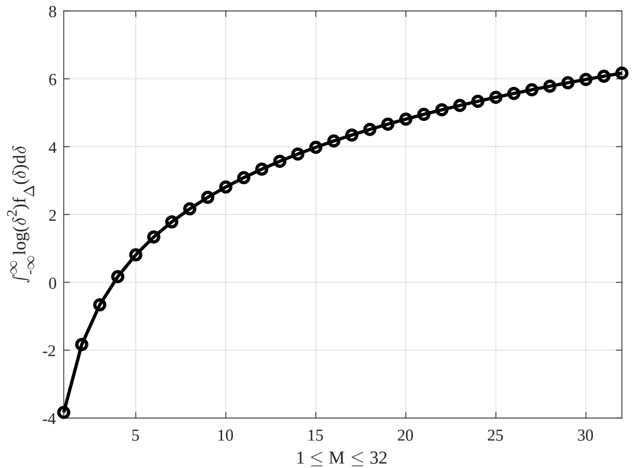

Fig. 7: Numerical solution for $\int_{-\infty}^{+\infty} \log\left(\delta^2\right) f_\Delta(\delta) d\delta$ with different number of sub-elements $1 \leq M \leq 32$, where $f_\Delta(\delta)$ has a Gaussian distribution with zero mean and variance of $\frac{M}{2}$.

- $\frac{M}{2}\log 3$: This term indicates the rate that can be achieved from the number of antenna sub-elements. It is interesting that without having multi-channel processing (*i.e.* joint processing), we still obtain the benefit multi-channel processing from the new proposed antenna structure with only one RF chain. The term $\frac{\log 3}{2}$ in this relation comes from having three different states for each sub-element across two times;
- $\frac{\alpha|\mathcal{K}|}{8}\log 3N$: This term indicates the rate achieved through the path-loss exponent and the frequency reuse factor which can help the receivers reduce the effect of of interference signals;
- $-\frac{|\mathcal{K}|}{4}\log\left(|\mathcal{K}|-1\right) - \frac{1.5(|\mathcal{K}|-1)}{2}\log 3$: This term represents the negative impact of interfering signals in the transmission environment which reduces the chance of finding proper channel condition at the receivers.

C. Outage capacity analysis

In this subsection, we analyze the outage capacity of our technique for different values of P_t. We define $(1-\epsilon)$ outage capacity for each user as follows:

$$C_{1-\epsilon} = \left\{R_t : P\left(R_t \geq C_h\right) \geq 1-\epsilon\right\}, \tag{35}$$

where R_t is the transmission rate in which there exist a state among $\frac{3^M-1}{2}$ different states with channel capacity of C_h with the probability greater than $1-\epsilon$. If we assume Gaussian distribution for $f_\Delta(\delta)$ with variance of $\frac{M}{2}\sigma_H^2$, the outage capacity can be calculated as follows:

$$C_{1-\epsilon} = \frac{1}{4}\log\left(1 + \frac{\Delta_\epsilon^2 P_t/R^\alpha}{P_n + \delta_{\max}^2\left(\frac{|\mathcal{K}-1|}{(R\sqrt{3N})^\alpha}P_t\right)}\right), \tag{36}$$

where Δ_ϵ is a positive-valued Δ for which $1 - \int_{-\Delta_\epsilon}^{\Delta_\epsilon} f_\Delta(\delta)d\delta \geq 1-\epsilon$. From the first lemma, if we consider Gaussian distribution with variance $\frac{M}{2}\sigma_H^2$ for $f_\Delta(\delta)$, the value of Δ_ϵ for specific value of ϵ can be calculated using the inverse of Q-function as follows:

$$\Delta_\epsilon = \sqrt{\frac{M}{2}}\sigma_H Q^{-1}\left(\frac{1-\epsilon}{2}\right). \tag{37}$$

VI. Search Algorithm

In the previous section, we proved that using our antenna structure it is possible to (almost surely) create conditions to align most of interference signal power to within a small value $\delta_{\max}$. In order to materialize this scheme, we need to search among 3^M different reception sates to find the best switching state at each receiver. For cellular wireless network applications, we typically engage with not more than 3 interference signals and choosing $M = 8$ is sufficient for our results. Therefore, in this small practical case, our scheme can be implemented using a brute-force search algorithm to go through $\frac{3^8-1}{2} = 3280$ points to minimize the effect of interference signals and maximize the desired signal power. However, when networks are dense and we engage with more users, the brute-force search becomes impractical.

Before we discuss our search algorithm, we define the optimization problem this algorithm needs to solve. From our system model and definitions, let $\bar{\gamma}^{[i]} = \left(\gamma_1^{[i]}, \gamma_2^{[i]}, \ldots, \gamma_M^{[i]}\right)$ be a vector where $\gamma_j^{[i]} \in \{-1, 0, 1\}$. At RX_i, the goal is to:

$$\max_{\bar{\gamma}^{[i]}} |h_{1i}^{[i]}\gamma_1^{[i]} + h_{2i}^{[1]}\gamma_2^{[i]} + \ldots h_{Mi}^{[i]}\gamma_M^{[i]}|, \tag{38}$$

while

$$|h_{1j}^{[i]}\gamma_1^{[i]} + h_{2j}^{[i]}\gamma_2^{[i]} + \cdots + h_{Mj}^{[i]}\gamma_M^{[i]}| \leq \delta_j,\ \ j \neq i, j \in \mathcal{K}, \tag{39}$$

where δ_j is a small positive real number. Another representation of this problem is as follows:

$$\max_{\bar{\gamma}^{[i]}} \frac{|\bar{\gamma}^{[i]}.\bar{\mathbf{H}}^{[ii]}|}{\sum_{j\in\mathcal{K}} |\bar{\gamma}^{[i]}.\bar{\mathbf{H}}^{[ij]}|}, \tag{40}$$

where in the above equation $\mathbf{U}.\mathbf{H}^{[i]}$ is the inner product between two vectors $\mathbf{U}$ and $\mathbf{H}^{[i]}$. We refer to

$$\frac{|\bar{\gamma}^{[i]}.\bar{\mathbf{H}}^{[ii]}|}{\sum_{j\in\mathcal{K}} |\bar{\gamma}^{[i]}.\bar{\mathbf{H}}^{[ij]}|} \tag{41}$$

as the *score function*.

Next, $\mathbf{H}^{[i]}$ can be expanded as follows:

$$\mathbf{H}^{[i]} = \left(h_1^{[i]}, h_2^{[i]}, \ldots, h_M^{[i]}\right). \tag{42}$$

It is straightforward to see that a simple brute-force search algorithm has a complexity of $\frac{3^M-1}{2}$, where the division by 2 comes from the fact that if $\bar{\gamma}_*^{[i]}$ is the optimum vector (except all-zero vector which is not a solution) for our optimization problem, then $-\bar{\gamma}_*^{[i]}$ is also an optimum vector. For large values of M, a brute-force search algorithm would be hard to implement.

A. Proposed search algorithm

We propose a state search method in which all switching states of the i^{th} receiver generate a set $\Gamma^{[i]} = \{\gamma_1^{[i]}, \gamma_2^{[i]}, \ldots, \gamma_M^{[i]}\},\ \gamma_j^{[i]} \in \{-1, 0, 1\}$. Our algorithm takes the following steps:
Step1: We generate $\binom{M}{L}$ different sates[2] of $\mathcal{F}_r^{[i]}, 1 \leq r \leq \binom{M}{L}$ where each state represents a set in which $|\mathcal{F}_r^{[i]}| = L$ and $\mathcal{F}_r^{[i]} \subset \Gamma^{[i]}$. In other words, we select a subset of size L of sub-elements at each receive antenna out of M different sub-elements.
Step2: At the first stage, using a simple brute-force search algorithm, we calculate the *score function* for different subsets of $\mathcal{F}_r^{(1)},\ 1 \leq r \leq \binom{M}{L}$ and we select N_s survived states (parents) with highest *score functions*. We call them survived subsets of $\{\mathcal{FS}_1^{(1)}, \mathcal{FS}_2^{(1)}, \ldots, \mathcal{FS}_{N_s}^{(1)}\}$ from the first stage. The complexity of this step is $\frac{3^L-1}{2}\binom{M}{L}$.
Note: When we calculate the *score function* for each state, we set all other elements in the set $\Gamma^{[i]} \setminus \mathcal{F}_r$ to zero.
Step 3: For every survived subset, we generate new subsets of $\mathcal{F}_r^{(2)},\ 1 \leq r \leq \binom{M-L}{L}$ from the remaining members of $\Gamma^{[i]} \setminus \mathcal{FS}_r^{(1)}$ which we refer to as the offsprings of the parents from the previous stage. Similar to previous step, we choose N_s of them with highest *score function* as new parents and survived subsets.
Step 4: We repeat step 3 until no subsets are left.

Fig. 8 shows our proposed searching algorithm to find a (possibly locally optimal) vector $\bar{\gamma}^{[i]}$ to maximize our *score function*.

[2]We assume M is divisible by L.

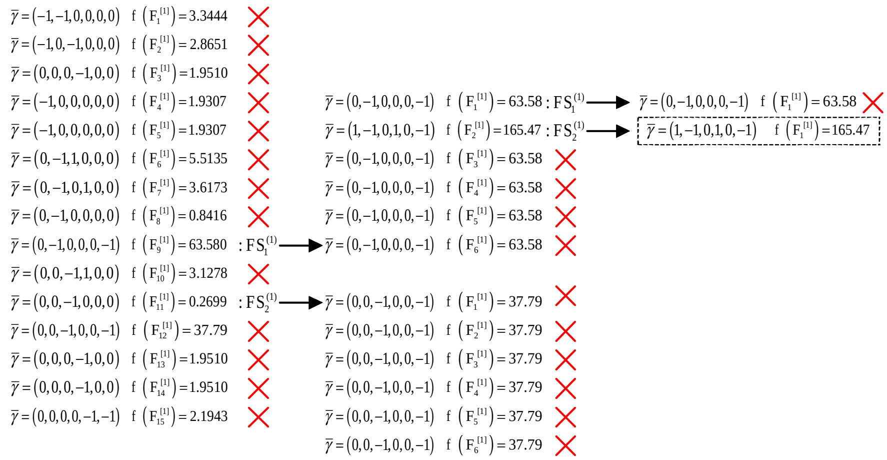

Fig. 8: The nodes with the arrows placed close to them indicate survived subsets and selected parents to generate offsprings. At each stage, N_s offsprings with the highest score function survive to continue the process. In this example, we used $N_s = L = 2$.

B. Complexity of the proposed search algorithm

As we discussed earlier, a simple brute-force search algorithm needs $\frac{3^M-1}{2}$ searching points to find the optimum solution. In this subsection, we analyze the complexity of our proposed search algorithm. At the first stage, we need to search among $\binom{M}{L}$ subsets where each subset using a simple brute-force algorithm needs to search among $\frac{3^L-1}{2}$ searching points. Therefore, at the first step we have a complexity of $\frac{3^L-1}{2}\binom{M}{L}$. At the second stage, we have N_s survived parents where for each parent we need to generate $\binom{M-L}{L}$ subsets. Similar to the previous stage, we need to search among $\frac{3^L-1}{2}$ searching point. Therefore, in this stage, we have a complexity of $N_s\frac{3^L-1}{2}\binom{M-L}{L}$. In general, during the i^{th} stage, we have the following complexity:

$$N_s \frac{3^L-1}{2}\binom{M-(i-1)L}{L}. \tag{43}$$

Finally, during the last stage, we have a complexity of $\frac{3^L-1}{2}$ (there is no choice to select among the subsets). Therefore, the total complexity of our algorithm can be calculated as follows:

$$\sum_{i=1}^{\frac{M}{L}-1} N_s \frac{3^L-1}{2}\binom{M-(i-1)L}{L} + \frac{3^L-1}{2}. \tag{44}$$

If the value of M has enough greater value than N_s and L, the order of complexity can be upper bounded from equation (44) as follows:

$$\sum_{i=1}^{\frac{M}{L}-1} N_s \frac{3^L-1}{2}\binom{M-(i-1)L}{L}+\frac{3^L-1}{2} \leq \sum_{i=1}^{\frac{M}{L}-1} N_s \frac{3^L-1}{2}\frac{(M-(i-1)L)^L}{L^L}+\frac{3^L-1}{2}$$
$$\approx \sum_{i=1}^{\frac{M}{L}-1} N_s \frac{3^L-1}{2}\left(\frac{M}{L}-(i-1)\right)^L+\frac{3^L-1}{2} \leq \mathcal{O}\left(M^{L+1}\right). \tag{45}$$

As an example, for $M = 32$, $L = 2$, and $N_s = 5$, the complexity of our proposed search algorithm at each receiver is 57104 which is 1.6×10^{10} times faster than the simple brute-force search algorithm.

As another example, consider a 3-user interference channel in which the channel vectors at the first receiver has the following form:

$$\bar{\mathbf{H}}^{[11]} = [+1.4090, +1.4172, +0.6715, -1.2075, +0.7172, +1.6302], \tag{46}$$

$$\bar{\mathbf{H}}^{[12]} = [+0.4889, +1.0347, +0.7269, -0.3034, +0.2939, -0.7873], \tag{47}$$

$$\bar{\mathbf{H}}^{[13]} = [+0.8884, -1.1471, -1.0689, -0.8095, -2.9443, 1.4384]. \tag{48}$$

Using the brute-force search algorithm with complexity of $3^6 = 729$ and setting $\bar{\gamma}^{[1]} = (-1, 1, 0, 1, -1, 0)$, we can reach a *score function* of $\frac{\Delta^2}{\delta^2} = 293.5$. Now, we want to test our proposed search algorithm by setting $N_s = 2$ and $L = 2$. In this case, the first receiver generate $\binom{6}{2} = 15$ subsets as follows:

$$\begin{aligned}
&\mathcal{F}_1^{[1]} = \{\gamma_1^{[1]}, \gamma_2^{[1]}\},\ \mathcal{F}_2^{[1]} = \{\gamma_1^{[1]}, \gamma_3^{[1]}\},\ \mathcal{F}_3^{[1]} = \{\gamma_1^{[1]}, \gamma_4^{[1]}\}\\
&\mathcal{F}_4^{[1]} = \{\gamma_1^{[1]}, \gamma_5^{[1]}\},\ \mathcal{F}_5^{[1]} = \{\gamma_1^{[1]}, \gamma_6^{[1]}\},\ \mathcal{F}_6^{[1]} = \{\gamma_2^{[1]}, \gamma_3^{[1]}\}\\
&\mathcal{F}_7^{[1]} = \{\gamma_2^{[1]}, \gamma_4^{[1]}\},\ \mathcal{F}_8^{[1]} = \{\gamma_2^{[1]}, \gamma_5^{[1]}\},\ \mathcal{F}_9^{[1]} = \{\gamma_3^{[1]}, \gamma_4^{[1]}\}\\
&\mathcal{F}_{10}^{[1]} = \{\gamma_2^{[1]}, \gamma_6^{[1]}\},\ \mathcal{F}_{11}^{[1]} = \{\gamma_3^{[1]}, \gamma_5^{[1]}\},\ \mathcal{F}_{12}^{[1]} = \{\gamma_3^{[1]}, \gamma_6^{[1]}\}\\
&\mathcal{F}_{13}^{[1]} = \{\gamma_4^{[1]}, \gamma_5^{[1]}\},\ \mathcal{F}_{14}^{[1]} = \{\gamma_4^{[1]}, \gamma_6^{[1]}\},\ \mathcal{F}_{15}^{[1]} = \{\gamma_5^{[1]}, \gamma_6^{[1]}\}.
\end{aligned} \tag{49}$$

For each subset above, using a simple brute-force search algorithm the receiver maximizes the *score function* $f\left(\mathcal{F}_j^{[1]}\right), 1 \leq j \leq \binom{6}{2} = 15$, and finds $N_s = 2$ of them with highest *score* *function*. In the above example the maximum score function for each of the above subset can be calculated as follows:

$$\begin{aligned}
&f\left(\mathcal{F}_1^{[1]}\right) = 3.3444, (-1,-1,0,0,0,0),\ f\left(\mathcal{F}_2^{[1]}\right) = 2.8651, (-1,0,-1,0,0,0),\\
&f\left(\mathcal{F}_3^{[1]}\right) = 1.9510, (0,0,0,-1,0,0),\ f\left(\mathcal{F}_4^{[1]}\right) = 1.9307, (-1,0,0,0,0,0),\\
&f\left(\mathcal{F}_5^{[1]}\right) = 1.9307, (-1,0,0,0,0,0),\ f\left(\mathcal{F}_6^{[1]}\right) = 5.5135, (0,-1,1,0,0,0),\\
&f\left(\mathcal{F}_7^{[1]}\right) = 3.6173, (0,-1,0,1,0,0),\ f\left(\mathcal{F}_8^{[1]}\right) = 0.8416, (0,-1,0,0,0,0),\\
&f\left(\mathcal{F}_9^{[1]}\right) = 63.580, (0,-1,0,0,0,-1),\ f\left(\mathcal{F}_{10}^{[1]}\right) = 3.1278, (0,0,-1,1,0,0),\\
&f\left(\mathcal{F}_{11}^{[1]}\right) = 0.2699, (0,0,-1,0,0,0),\ f\left(\mathcal{F}_{12}^{[1]}\right) = 37.7934, (0,0,-1,0,0,-1)\\
&f\left(\mathcal{F}_{13}^{[1]}\right) = 1.9510, (0,0,0,-1,0,0),\ f\left(\mathcal{F}_{14}^{[1]}\right) = 1.9510, (0,0,0,-1,0,0),\\
&f\left(\mathcal{F}_{15}^{[1]}\right) = 2.1943, (0,0,0,0,-1,-1). \qquad (50)
\end{aligned}$$

Given $N_s = 2$, $f\left(\mathcal{F}_9^{[1]}\right) = 63.580, \bar{\gamma}^{[1]} = (0,-1,0,0,0,-1)$ and $f\left(\mathcal{F}_{12}^{[1]}\right) = 37.7934, \bar{\gamma}^{[1]} = (0,0,-1,0,0,-1)$ are the survived parents. From the first survived state $\mathcal{FS}_9^{[1]} = (0,-1,0,0,0,-1)$, we have $\binom{6-N_s}{2} = 6,\ N_s = 2$ offspings as follows:

$$\begin{aligned}
&f\left(\mathcal{F}_1^{[1]}\right) = 63.58, (0,-1,0,0,0,-1),\ f\left(\mathcal{F}_2^{[1]}\right) = 165.4732, (1,-1,0,1,0,-1),\\
&f\left(\mathcal{F}_3^{[1]}\right) = 63.58, (0,-1,0,0,0,-1),\ f\left(\mathcal{F}_4^{[1]}\right) = 63.58, (0,-1,0,0,0,-1),\\
&f\left(\mathcal{F}_5^{[1]}\right) = 63.58, (0,-1,0,0,0,-1),\ f\left(\mathcal{F}_6^{[1]}\right) = 63.58, (0,-1,0,0,0,-1). \qquad (51)
\end{aligned}$$

From the survived state $\mathcal{FS}_{12}^{[1]} = (0,0,-1,0,0,-1)$, we have $\binom{6-N_s}{2} = 6,\ N_s = 2$ offsprings as follows:

$$\begin{aligned}
&f\left(\mathcal{F}_1^{[1]}\right) = 37.7934, (0,0,-1,0,0,-1),\ f\left(\mathcal{F}_2^{[1]}\right) = 37.7934, (0,0,-1,0,0,-1),\\
&f\left(\mathcal{F}_3^{[1]}\right) = 37.7934, (0,0,-1,0,0,-1),\ f\left(\mathcal{F}_4^{[1]}\right) = 37.7934, (0,0,-1,0,0,-1),\\
&f\left(\mathcal{F}_5^{[1]}\right) = 37.7934, (0,0,-1,0,0,-1),\ f\left(\mathcal{F}_6^{[1]}\right) = 37.7934, (0,0,-1,0,0,-1). \qquad (52)
\end{aligned}$$

From the above relations, we can determine two further survived parents of $f\left(\mathcal{F}_2^{[1]}\right) = 165.4732$, $\bar{\gamma}^{[1]} = (1,-1,0,1,0,-1)$ and $f\left(\mathcal{F}_1^{[1]}\right) = 63.58, \bar{\gamma}^{[1]} = (0,-1,0,0,0,-1)$ where each parent has one offspring. Finally, the *score function* is maximized by setting $\bar{\gamma}_*^{[1]} = (1,-1,0,1,0,-1)$ and the value of *score function* is 165.4732 with a complexity of 256 compared to $3^6 = 729$ for the brute-force algorithm. The gap between our proposed algorithm and the brute-force algorithm grows quickly as M increases.

C. Random search

In this case, we randomly choose different $\bar{\gamma}^{[i]}$'s at each receiver and we select a vector which satisfies the minimum SINR condition at that receiver. When the value of M is large enough, we will show in the numerical results that the number of local maximums is sufficiently large to satisfy our conditions.

VII. Numerical and simulation results

In this section, we numerically analyze the performance of our proposed alignment strategy using our antenna structure. In our simulation results, we assume Rayleigh fading channels in which the real and the imaginary parts of the channel gains are modeled by independent and identically distributed zero-mean Gaussian processes. Since the real and the imaginary parts are independent of each other, our technique can be modified using simple 90 degrees phase shifter elements and RF switches. Therefore, we analyze only the real part of channel coefficients and the results can be generalized to complex channels. Basically, in all our simulations, we assume that there exist real-valued channel coefficients with Gaussian distribution among transmitters and receivers sub-elements.

Figure 9 shows a comparison between Monte Carlo simulation with 1000 tries and our approximation of relation (53), where we have:

$$p\left(|\bar{\mathbf{H}}^{[ij]}.\bar{\gamma}^{[j]}| < \delta\right) \approx \frac{2}{\sqrt{\pi M}}\frac{\delta_{\max}}{\sigma_H},\ j \text{ is constant.} \tag{53}$$

We observe that our approximation traces the simulation results within a small margin when $0.01 \leq \delta \leq 0.1$. As it is indicated in this figure, our approximate relation becomes more accurate for smaller values of δ.

Figure 10 shows our average transmission rate for a 4-user interference channel with $M = 16$ sub-elements at each receiver. In this figure, the red solid curve indicates the sum rate of a $4-$user interference channel with perfect CSI, the dashed blue curve indicate the sum rate of this channel using our antenna structure and a simple brute-force algorithm. From (34), a lower-bound on the saturation rate can be calculated as follows:

$$C_{\text{avg}} \geq \int_{-\infty}^{+\infty} \frac{|\mathcal{K}|}{4}\log\left(\delta^2\right) f_\Delta(\delta)d\delta + \frac{M-1.5(|\mathcal{K}|-1)}{2}\log 3 + \frac{\alpha|\mathcal{K}|}{8}\log 3N - \frac{|\mathcal{K}|}{4}\log\left(|\mathcal{K}|-1\right) \tag{54}$$

$$= \frac{4\times 4}{4} + \frac{16-1.5\times 3}{2}\log 3 - \frac{4}{4}\log 52 = 11.66, \tag{55}$$

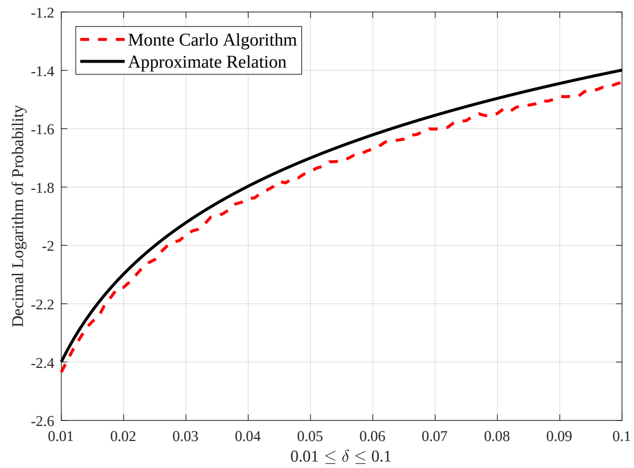

Fig. 9: Comparison between our approximation of (53) and a Monte Carlo simulation with $M = 8$, $\sigma_H = 1$, and 1000 trials.

which matches what we observe in Figure 10. We should note that since in this case we do not use the interference reduction technique of cellular networks, the term $\frac{\alpha|\mathcal{K}|}{8} \log 3N$ does not play a role in our relation (all the interference signals are received at the same power level).

As it is indicated our antenna structure can help the receivers to trace the sum rate of original IA scheme in applicable SNR region $(\mathrm{SNR} \leq 40\mathrm{dB})$ without accessing channel state information at the transmitters. Since the simple brute-force search increases the complexity, we use our proposed algorithm, and as indicated in Figure 10(a) for $N_s = 2$ and $L = 4$, the number of trials is 1.8×10^4 compared to the brute-force search with 2.15×10^7 trials. This faster solution results in an acceptable 5dB performance degradation. We observe that our technique traces the perfect interference alignment sum-rate outer-bound for a wide range of SNR values. We note that the perfect interference alignment scheme works for high SNR values and the bound is only included for comparison.

Figure 10(b) shows the outage capacity of our proposed strategy for different values of $1 - \epsilon$. Not surprisingly, when $\epsilon = 0$, we cannot find any value for R_t (transmission rate) in which the receiver can almost surely recover the transmitted data. Therefore, in this case, the value of $C_{1-\epsilon}$ is zero. As ϵ moves away from zero, the value of $C_{1-\epsilon}$ starts increasing.

Table II and III show the performance and complexity of our proposed search algorithm compared to random search algorithm with complexity of $\frac{3^8-1}{2}$ and simple brute-force algorithm with the complexity of $\frac{3^M-1}{2}$. For $K = 4$ users, our approach exhibits good performance while reducing the complexity of search algorithm drastically. For $M = 16$, our sum rate has a

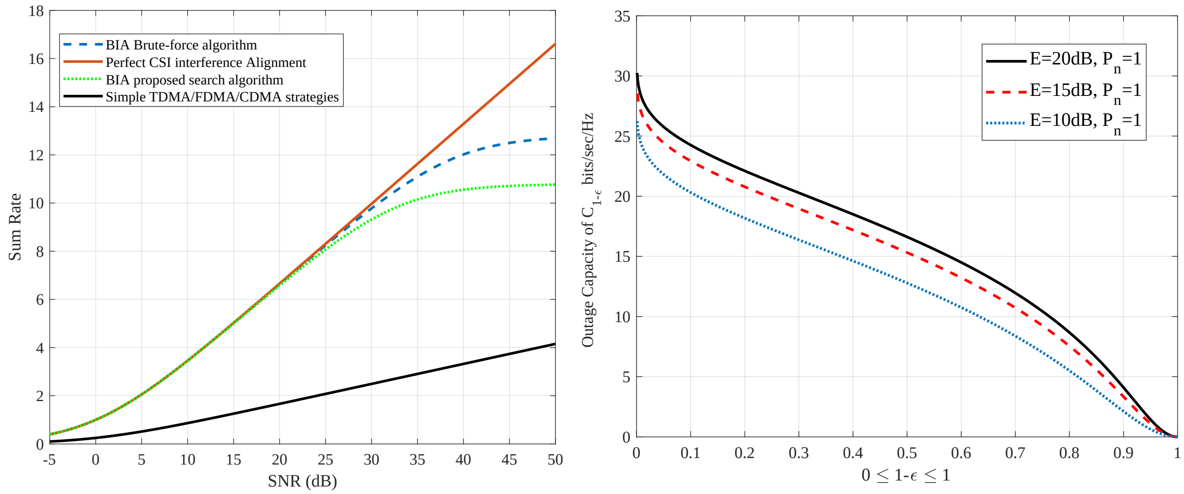

(a) **(b)**

Fig. 10: (a) Comparison between our proposed strategy and interference alignment with perfect CSI in a 4-user IC; (b) The outage capacity as a function of $(1-\epsilon)$ for $M = 12$ and $K = 6$ users and varying transmission power ($\mathcal{E} = 10, 15, 20\mathrm{dB}$).

TABLE I: Example of 4-user IC and the highest *score function* value

K=4	$M = 8$	$M = 16$	$M = 24$
Brute-force algorithm	$\max \frac{\Delta^2}{\delta^2} = 100$	$\max \frac{\Delta^2}{\delta^2} = 16 \times 10^4$	$\max \frac{\Delta^2}{\delta^2} = 9 \times 10^6$
Proposed strategy	$\max \frac{\Delta^2}{\delta^2} = 100$	$\max \frac{\Delta^2}{\delta^2} = 7.5 \times 10^4$	$\max \frac{\Delta^2}{\delta^2} = 3 \times 10^6$
Random search	$\max \frac{\Delta^2}{\delta^2} = 100$	$\max \frac{\Delta^2}{\delta^2} = 3 \times 10^3$	$\max \frac{\Delta^2}{\delta^2} = 8 \times 10^4$

saturation point around $48\mathrm{dB}$ and has a complexity of 19000 which even with basic processors at $60\mathrm{MHz}$ can be calculated within 0.3ms. Considering channel coherence time of $\frac{c}{fv} = 6.25\mathrm{ms}$ for a receiver with a speed of $v = 30\mathrm{m/sec}$ and operation frequency of $f = 1.6\mathrm{GHz}$, the search algorithm overhead is a negligible part of signaling.

TABLE II: Complexity of different schemes compared to our scheme with $L = 4$ and $N_s = 2$

K=4	$M = 8$	$M = 16$	$M = 24$
Brute-force algorithm	$\frac{3^8-1}{2}$	$\frac{3^{16}-1}{2}$	$\frac{3^{24}-1}{2}$
Proposed strategy	5640	1.9×10^4	1.4×10^6
Random search	$\frac{3^8-1}{2}$	$\frac{3^8-1}{2}$	$\frac{3^8-1}{2}$

VIII. Conclusion and future work

In this paper, we proposed a distributed blind interference management strategy in $K-$user ICs that exploits the receiver-end diversity created by our proposed antenna. A major difference between our antenna and other multiple-antenna structures is that it can be used without using joint processing or multiple RF chains. The proposed scheme allows transceivers to achieve higher average sum-rate without accessing CSI at the transmitters, and matches the promised high-SNR gains of Interference Alignment for finite SNR values. We designed our scheme such that interference signals align to within a small margin. We showed that when the number of sub-elements at the receivers increases, the chance of finding proper channel conditions to eliminate most of interfering signal power increases. We then analyzed the average achievable sum-rate of our approach, and we proposed an efficient algorithm to search among different reception states. We showed that by a small sacrifice in SINR, we can find proper states with lower complexity. Through numerical analysis, we showed that our new approach enables interference mitigating without the main drawbacks of prior results. One can extend the results of this paper for other types of interference channels and channel networks with different topology or protocols to improve data reception rate which is the main bottleneck in today wireless networks. Another step to improve the performance of the system is to analyze the antenna structure with different types of antenna sub-elements or increase the number of reception switching state with some phase shifter or attenuator elements. It is obvious by increasing the number of reception states the chance of finding proper switching state at receivers increases and we expect better performance.

Appendix A
6-user example

The receivers have the random positions as follows:

$$\begin{aligned}
\left(x_r^{[1]}, y_r^{[1]}, z_r^{[1]}\right) &= \lambda\left(-96.7399, -53.9274, -80.9076\right) \\
\left(x_r^{[2]}, y_r^{[2]}, z_r^{[2]}\right) &= \lambda\left(-43.8800, -1.83620, -57.1747\right) \\
\left(x_r^{[3]}, y_r^{[3]}, z_r^{[3]}\right) &= \lambda\left(-11.8133, -84.3595, -51.7978\right) \\
\left(x_r^{[4]}, y_r^{[4]}, z_r^{[4]}\right) &= \lambda\left(-33.0825, -14.4477, -87.9388\right) \\
\left(x_r^{[5]}, y_r^{[5]}, z_r^{[5]}\right) &= \lambda\left(-80.9567, -35.5235, -41.0493\right) \\
\left(x_r^{[6]}, y_r^{[6]}, z_r^{[6]}\right) &= \lambda\left(-63.1083, -62.3728, -77.3812\right),
\end{aligned} \tag{56}$$

The transmitters have the following random positions:

$$\begin{aligned}
\left(x_t^{[1]}, y_t^{[1]}, z_t^{[1]}\right) &= \lambda\left(-61.5381, -41.7014, -74.8194\right) \\
\left(x_t^{[2]}, y_t^{[2]}, z_t^{[2]}\right) &= \lambda\left(-70.9559, -38.2909, -73.4719\right) \\
\left(x_t^{[3]}, y_t^{[3]}, z_t^{[3]}\right) &= \lambda\left(-17.5624, -1.73370, -26.9751\right) \\
\left(x_t^{[4]}, y_t^{[4]}, z_t^{[4]}\right) &= \lambda\left(-65.6123, -41.5931, -89.2231\right) \\
\left(x_t^{[5]}, y_t^{[5]}, z_t^{[5]}\right) &= \lambda\left(-9.36920, -12.0346, -18.2239\right) \\
\left(x_t^{[6]}, y_t^{[6]}, z_t^{[6]}\right) &= \lambda\left(-73.9272, -40.5644, -97.7487\right),
\end{aligned} \tag{57}$$

Appendix B
Proof of the first lemma

Proof: The vector $\bar{\gamma}^{[i]} = \left(\gamma_1^{[i]}, \ldots, \gamma_M^{[i]}\right)$ has 3^M different shapes in which $\gamma_k^{[i]} \in \{-1, 0, 1\}$. The inner product of two vectors $\bar{\mathbf{H}}^{[ij]}$ and $\bar{\gamma}^{[i]}$ can be expanded as follows:

$$\bar{\mathbf{H}}^{[ij]}.\bar{\gamma}^{[i]} = \sum_{k=1}^{M} h_k^{[ij]} \gamma_k^{[j]}. \tag{58}$$

Therefore, we have:

$$\operatorname{var}\left(\bar{\mathbf{H}}^{[ij]}.\bar{\gamma}^{[i]}\right) = \operatorname{var}\left(\sum_{k=1}^{M} h_k^{[ij]} \gamma_k^{[i]}\right) = \sum_{k=1}^{M} \operatorname{var}\left(h_k^{[ij]}\right) |\gamma_k^{[i]}| = \sigma_H^2 \sum_{k=1}^{M} |\gamma_k^{[i]}| \tag{59}$$

If we consider uniform distribution among different state of the vector $\bar{\gamma}^{[i]}$, the average variance of $\operatorname{var}\left(\bar{\mathbf{H}}^{[ij]}.\bar{\gamma}^{[i]}\right)$ can be calculated as follows:

$$\bar{\operatorname{var}}\left(\bar{\mathbf{H}}^{[ij]}.\bar{\gamma}^{[i]}\right) = \mathbb{E}\left(\sigma_H^2 \sum_{k=1}^{M} |\gamma_k^{[i]}|\right) \tag{60}$$

$$= \sigma_H^2 \sum_{l=0}^{M} p\left(\sum_{k=1}^{M} |\gamma_k^{[i]}| = l\right) l,\ \ 0 \le l \le M. \tag{61}$$

If we consider uniform distribution among different switching states, the value of $p\left(\sum_{k=1}^{M} |\gamma_k^{[i]}| = l\right)$ can be calculated from $\frac{\binom{M}{M-l}}{2^M}$. In which, the value of $\binom{M}{M-l}$ counts the number of states in which the vector $\bar{\gamma}^{[i]}$ contains $M - l$ zeros and 2^M indicates total number of states for $|\bar{\gamma}^{[i]}|$ which contains zero or one. Therefore, we can conclude that:

$$\bar{\operatorname{var}}\left(\bar{\mathbf{H}}^{[ij]}.\bar{\gamma}^{[i]}\right) = \frac{\sum_{l=0}^{M} \binom{M}{M-l} l}{2^M} \sigma_H^2, \tag{62}$$

if we substitute $M-l$ with l', then:

$$\bar{\text{var}}\left(\bar{\mathbf{H}}^{[ij]}.\bar{\gamma}^{[i]}\right)=\frac{\sum_{l'=0}^{M}\binom{M}{l'}(M-l')}{2^M}\sigma_H^2=\frac{M}{2}\sigma_H^2 \tag{63}$$

which completes the proof. ■

Appendix C
Proof of the second lemma

Proof: As it discussed in the previous lemma for different vectors, $\bar{\gamma}^{[i]}$, the distribution of $\bar{\mathbf{H}}^{[ij]}.\bar{\gamma}^{[i]}$ can be approximated by Gaussian distribution with zero mean and variance V. So, we have:

$$p\left(|\bar{\mathbf{H}}^{[ij]}.\bar{\gamma}^{[i]}|<\delta\right)=\int_{-\delta}^{\delta}\frac{1}{\sqrt{2\pi V}}e^{-\frac{r^2}{2V}}dr \tag{64}$$

$$\overset{(a)}{\approx}\int_{-\delta}^{\delta}\frac{1}{\sqrt{2\pi V}}\left(1-\frac{r^2}{2V}+O\left(\frac{r^4}{V^3}\right)\right)dr \tag{65}$$

$$=\frac{2}{\sqrt{2\pi}}\frac{\delta}{\sigma}-\frac{2}{3\sqrt{2\pi}}\frac{\delta^3}{\sigma^3}+O\left(\frac{\delta^5}{\sigma^5}\right) \tag{66}$$

where the approximation (a) comes from the Taylor series expansion of the term $e^{-\frac{r^2}{2V}}$ and in all the above equations σ is equal to $\sqrt{V}$. ■

References

[1] A. E. Gamal and M. Costa, "The capacity region of a class of deterministic interference channels," *IEEE Transactions on Information Theory*, vol. 28, pp. 343–346, March 1982.

[2] R. Etkin, D. Tse, and H. Wang, "Gaussian interference channel capacity to within one bit," *IEEE Transactions on Information Theory*, vol. 54, pp. 5534–5562, December 2008.

[3] A. Vahid, M. Maddah-Ali, and A. S. Avestimehr, "Capacity results for binary fading interference channels with delayed CSIT," *IEEE Transactions on Information Theory*, vol. 60, no. 10, pp. 6093–6130, 2014.

[4] A. Vahid and R. Calderbank, "Throughput region of spatially correlated interference packet networks," *IEEE Transactions on Information Theory*, vol. 65, no. 2, pp. 1220–1235, 2019.

[5] Te Han and K. Kobayashi, "A new achievable rate region for the interference channel," *IEEE Transactions on Information Theory*, vol. 27, pp. 49–60, January 1981.

[6] A. El Gamal and Y.-H. Kim, *Network information theory*. Cambridge university press, 2011.

[7] T. S. Rappaport, G. R. MacCartney, M. K. Samimi, and S. Sun, "Wideband millimeter-wave propagation measurements and channel models for future wireless communication system design," *IEEE Transactions on Communications*, vol. 63, pp. 3029–3056, Sep. 2015.

[8] S. W. Choi, S. A. Jafar, and S.-Y. Chung, "On the beamforming design for efficient interference alignment," *IEEE Communications Letters*, vol. 13, no. 11, pp. 847–849, 2009.

[9] M. Johnny and M. R. Aref, “An efficient precoder size for interference alignment of the K-user interference channel,” *IEEE Communications Letters*, vol. 21, no. 9, pp. 1941–1944, 2017.

[10] B. Nosrat-Makouei, J. G. Andrews, and R. W. Heath, “Mimo interference alignment over correlated channels with imperfect csi,” *IEEE Transactions on Signal Processing*, vol. 59, pp. 2783–2794, June 2011.

[11] M. A. Maddah-Ali and D. N. Tse, “Completely stale transmitter channel state information is still very useful,” *IEEE Transactions on Information Theory*, vol. 58, pp. 4418–4431, July 2012.

[12] H. Maleki, S. A. Jafar, and S. Shamai, “Retrospective interference alignment over interference networks,” *IEEE Journal of Selected Topics in Signal Processing*, vol. 6.3, pp. 228–240, June 2012.

[13] A. Vahid, M. A. Maddah-Ali, and A. S. Avestimehr, “Approximate capacity region of the MISO broadcast channels with delayed CSIT,” *IEEE Transactions on Communications*, vol. 64, no. 7, pp. 2913–2924, 2016.

[14] D. Castanheira, A. Silva, and A. Gameiro, “Retrospective interference alignment: Degrees of freedom scaling with distributed transmitters,” *IEEE Transactions on Information Theory*, vol. 63, pp. 1721–1730, March 2017.

[15] A. Vahid, M. A. Maddah-Ali, and A. S. Avestimehr, “Capacity results for binary fading interference channels with delayed CSIT,” *IEEE Transactions on Information Theory*, vol. 60, no. 10, pp. 6093–6130, 2014.

[16] S. A. Jafar, “Blind interference alignment,” *IEEE Journal of Selected Topics in Signal Processing*, vol. 6, no. 3, pp. 216–227, 2012.

[17] M. Johnny and M. R. Aref, “BIA for the K-user interference channel using reconfigurable antenna at receivers,” *IEEE Transactions on Information Theory*, vol. 66, pp. 2184–2197, April 2020.

[18] G. Caire and S. Shamai, “On achievable rates in a multi-antenna gaussian broadcast channel,” in *Proceedings. 2001 IEEE International Symposium on Information Theory (IEEE Cat. No.01CH37252)*, pp. 147–, June 2001.

[19] S. A. Jafar, “Too much mobility limits the capacity of wireless ad hoc networks,” *IEEE Transactions on Information Theory*, vol. 51, pp. 3954–3965, Nov 2005.

[20] T. Gou, C. Wang, and S. A. Jafar, “Aiming perfectly in the dark-blind interference alignment through staggered antenna switching,” *IEEE Transactions on Signal Processing*, vol. 59, pp. 2734–2744, June 2011.

[21] M. Johnny and M. R. Aref, “Sum degrees of freedom for the k-user interference channel using antenna switching,” in *WSA 2017; 21th International ITG Workshop on Smart Antennas*, pp. 1–6, March 2017.

[22] B. Nazer, M. Gastpar, S. A. Jafar, and S. Vishwanath, “Ergodic interference alignment,” *IEEE Transactions on Information Theory*, vol. 58, no. 10, pp. 6355–6371, 2012.

[23] A. Leshem and U. Erez, “Ergodic spatial nulling for achieving interference free rates,” in *2019 IEEE International Symposium on Information Theory (ISIT)*, pp. 1292–1296, 2019.

[24] M. Johnny and A. Vahid, “Embedding information in radiation pattern fluctuations,” in *IEEE International Symposium on Information Theory (ISIT)*, 2020.

[25] M. Johnny and A. Vahid, “Exploiting coherence time variations for opportunistic blind interference alignment,” *IEEE Transactions on Communications*, 2020.

[26] A. G. Davoodi and S. A. Jafar, “Aligned image sets under channel uncertainty: Settling conjectures on the collapse of degrees of freedom under finite precision CSIT,” *IEEE Transactions on Information Theory*, vol. 62, no. 10, pp. 5603–5618, 2016.

[27] T. S. Rappaport *et al.*, *Wireless communications: principles and practice*, vol. 2. prentice hall PTR New Jersey, 1996.